EuroSun 2026

STATE-SCALE ROOFTOP PHOTOVOLTAIC POTENTIAL MAPPING FROM OPEN LIDAR DATA WITH SHADING-DRIVER DECOMPOSITION AND ROOF-SUPERSTRUCTURE FILTERING: NORTH RHINE-WESTPHALIA (GERMANY)

Summary

Municipal PV strategies increasingly rely on solar cadastres, yet many products remain black boxes regarding which physical constraints suppress deployable roof area. We present a state-scale LiDAR/LoD2 workflow that maps technical rooftop PV potential while separating persistent shading drivers – building-to-building (G2G), tree-to-building (B2G) and roof-superstructure self-shading (E2G) – and storing intermediate layers in a geo-semantic database. Applied to ~10 million buildings in North Rhine-Westphalia (NRW), 1,250 km^2 gross roof area reduces to 432.97 km^2 deployable module footprint (≥7 m^2), corresponding to 62.94 GWp and 51.38 TWh·a^{-1} under explicit conversion assumptions. Benchmarking against the NRW cadastre baseline [5] and Energieatlas NRW [4] illustrates how non-harmonised power-density and yield assumptions distort comparisons.

Keywords: Rooftop PV, solar cadastre, LiDAR, 3D shading, roof superstructures, district energy planning

Field of application for the findings: Solar cadastres and district energy planning (technical rooftop PV potential; loss diagnostics for targeted interventions)

Addressed audience: Municipal/regional planners, solar cadastre operators, PV analysts, GIS/remote sensing researchers

1. Introduction & Methodology

Rooftop PV is expanding rapidly and is increasingly embedded in municipal heat and electricity transition strategies. Planning instruments therefore rely on rooftop potential maps to screen districts, prioritise campaigns and design supporting measures. However, absolute potentials depend strongly on how (i) 3D shading from buildings and vegetation and (ii) rooftop superstructures and module layout constraints are represented. Many cadastres provide a single number per roof or district without transparent loss diagnostics, making it difficult to decide whether local interventions should focus on vegetation trimming, roof refurbishment, or mitigation of inter-building shading. Reviews of solar cadastres highlight that many platforms remain opaque with respect to assumptions and dominant loss mechanisms [1]. At the same time, building-level rooftop PV potential

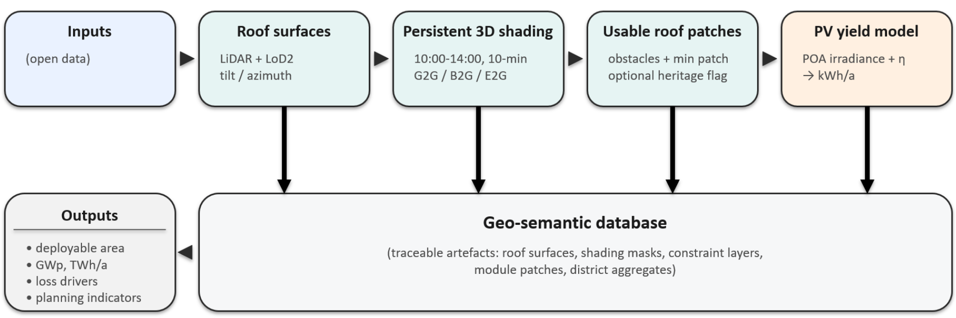

Fig. 1: Statewide reduction chain across driver-resolved shading constraints and module-layout rules.

Tab. 1: Statewide totals and normalised indicators (this work vs. baseline references).

Reference	Area [km^2]	Capacity [GWp]	Electricity [$TWh \cdot a^{-1}$]	Power density [$Wp \cdot m^{-2}$]	Specific yield [$kWh \cdot kWp^{-1}$]
This work ($\geq$7 m^2)	432.97	62.94	51.38	145	816
LANUV baseline (2018)	483.00	81.40	68.40	169	840
Energieatlas NRW (03/2025)	387.00	–	67.80	–	–

mapping is gaining prominence at European scale [2]. Complementary deep-learning-based PV panel mapping can provide empirical cross-checks but raises questions about transferability and bias [3]. Recent reviews synthesise LiDAR processing pipelines for solar cadastres [6]. Unlike learned pipelines, the present approach provides physically interpretable, driver-attributable loss decomposition at state scale. The workflow links airborne laser scanning (ALS) point clouds to a semantic Level of Detail 2 (LoD2) 3D building model with standardized, realistic roof shapes and orientations based on actual footprints. Roof points are segmented into planar roof surfaces with tilt/azimuth attributes and stored together with building, vegetation and administrative entities in a geo-semantic database that preserves intermediate artefacts (roof patches, shadow masks, usable-area layers) for auditability. To balance physical representativeness and state-scale tractability, 3D shadow projections are sampled in an energy-dominant window (10:00–14:00 local time, Δt=10 min) for each day of the year. Rather than reconstructing the full annual shading chronology, this energy-weighted sampling focuses on hours that dominate plane-of-array irradiation and is therefore intended as a conservative geometric suitability filter. Per driver, time-step shadow polygons are aggregated into persistent shading masks by retaining sub-areas shaded in $\geq$33% of samples; the threshold acts as a geometric robustness criterion that filters transient artefacts while preserving recurrent obstruction. Driver shares are reported as sequentially removed roof-area fractions in the fixed order G2G$\rightarrow$B2G$\rightarrow$E2G (order-dependent by design). Roof superstructures affect technical potential through two distinct mechanisms: (i) foof-superstructure self-shading and (ii) the roof area they occupy (roof-obstacle footprints, excluded separately in the reduction chain). Solar positions are computed with the NREL Solar Position Algorithm [9]. Annual plane-of-array irradiation is computed with the Perez transposition model [7] and converted to electricity with a constant module efficiency (η=17%); installed capacity is derived from module footprint using a consistent power-density assumption (Tab. 1).

2. Results & Conclusion

Fig. 1 summarises the statewide reduction chain from gross roof area to deployable module area. Across NRW, 1,250 km^2 gross roof area is reduced to 747 km^2 shadow-free roof area after driver-resolved shading constraints (G2G+B2G+E2G), to 633 km^2 after excluding roof-obstacle footprints, and to 432.97 km^2 deployable module area after module-layout rules ($\geq$7 m^2). A stricter 12 m^2 minimum patch threshold reduces deployable area to 395.72 km^2 (-8.6%). Driver attribution across 53 districts indicates that roof-superstructure self-shading (E2G) dominates *shading-induced* reductions on average (mean 57.8%, std 9.3%), followed by building-to-building shading (G2G; mean 32.8%, std 8.4%) and vegetation shading (B2G; mean 9.4%, std 4.1%). Ranges are wide (E2G 34.3–83.2%; G2G 10.5–61.9%), highlighting that mitigation strategies are district-specific. Tab. 1 benchmarks statewide totals against the NRW solar cadastre baseline (LANUV 2018; now operated by LANUK) and the updated Energieatlas NRW (03/2025). Reporting normalised indicators ($Wp \cdot m^{-2}$, $kWh \cdot kWp^{-1}$) helps disentangle differences due to geometric constraints from differences in conversion assumptions (e.g., module power density or efficiency). Tab. 2 disaggregates the statewide results into NRW's planning regions and

Tab. 2: Regional breakdown of deployable module area, capacity and yield (baseline values in parentheses).

Region	Area [km^2]	Capacity [GWp]	Electricity [$TWh \cdot a^{-1}$]
Arnsberg	38.80 (38)	5.82 (6.4)	4.32 (5.1)
Detmold	65.41 (69)	9.57 (11.7)	7.58 (9.6)
Düsseldorf	70.46 (99)	10.67 (16.7)	9.06 (14.4)
Köln	103.22 (118)	14.71 (19.9)	12.55 (17.0)
Münster	54.94 (60)	7.94 (10.1)	6.14 (8.3)
Regionalverband Ruhr	100.12 (99)	14.23 (16.7)	11.73 (13.9)
NRW total	432.97 (483)	62.94 (81.4)	51.38 (68.4)

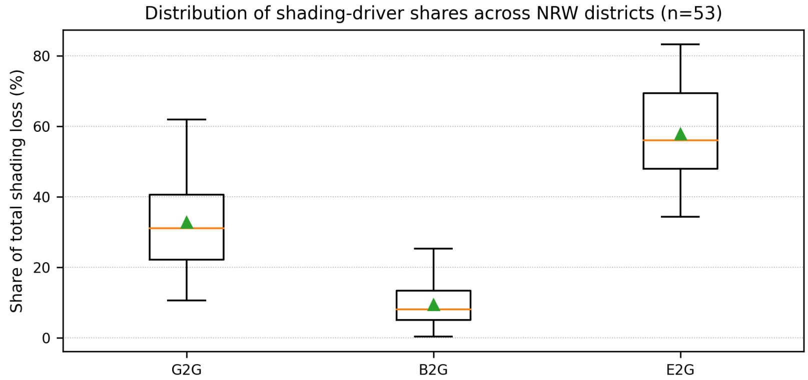

Fig. 2: Distribution of district-level shading-driver contributions (sequential shares; G2G→B2G→E2G). (G2G: buildings; B2G: trees; E2G: roof-superstructure self-shading).

highlights where absolute potentials concentrate. The planning region Cologne reaches 103.22 km^2 deployable module area, corresponding to 14.71 GWp and 12.55 $TWh{\cdot}a^{-1}$, followed closely by the Ruhr region with 100.12 km^2, 14.23 GWp and 11.73 $TWh{\cdot}a^{-1}$. Fig. 2 visualises the district-level distribution of sequential driver shares. While E2G dominates on average, the spread indicates substantial inter-district heterogeneity: in several dense districts, G2G becomes comparable to E2G, whereas B2G remains secondary for most districts. By exposing whether buildings (G2G), vegetation (B2G) or roof-superstructure self-shading (E2G) dominate shading-induced reductions, statewide totals become actionable diagnostics for planners. Remaining uncertainties due to surface-model quality and seasonal vegetation should be treated explicitly when transferring the approach to other regions [8].

References

[1] M. Giorio et al. Interactive platforms for solar energy planning in smart cities: A state-of-the-art review of solar cadasters. *Solar Energy*, 287:113227, 2025.

[2] G. Kakoulaki, N. Taylor, et al. Communication on the potential of applied pv in the eu. *EPJ Photovoltaics*, 15:2, 2024.

[3] R. Kasmi, L. Dubus, Y.-M. Saint-Drenan, and P. Blanc. Space-scale exploration of the poor reliability of deep learning models: The case of the remote sensing of rooftop photovoltaic systems. *Environmental Data Science*, 4:e22, 2025.

[4] LANUK. Energieatlas nrw: Potenziale der solarenergie in nrw (status 03/2025). Landesamt für Natur, Umwelt und Klima Nordrhein-Westfalen, 2025. Available at: `https://tinyurl.com/2nccpyc6` (accessed 2026-02-22).

[5] LANUV. Erstes landesweites solarkataster für nordrhein-westfalen ist online (press release, 8 nov 2018). Landesamt für Natur, Umwelt und Verbraucherschutz Nordrhein-Westfalen (LANUV), 2018. Available at: `https://tinyurl.com/22m8fb7v` (accessed 2026-02-22).

[6] R. Mahir, R. Bachour, et al. Processing airborne lidar point cloud for solar cadastres: A review. *Applied Energy*, 382:125325, 2025.

[7] R. Perez, P. Ineichen, R. Seals, J. Michalsky, and R. Stewart. Modeling daylight availability and irradiance components from direct and global irradiance. *Solar Energy*, 44(5):271–289, 1990.

[8] J. Polo and F. P. García. Solar potential uncertainty in building rooftops as a function of digital surface model quality. *Remote Sensing*, 15(3):567, 2023.

[9] I. Reda and A. Andreas. Solar position algorithm for solar radiation applications. Technical Report NREL/TP-560-34302, National Renewable Energy Laboratory (NREL), 2008. Available at: `https://tinyurl.com/y4kv23d6` (accessed 2026-02-22).